Submitted to Journal of Crystal Lattice Defects

UCRL-19117
Preprint

c.2

RECEIVED
LAW...
RADIATION LA...
FEB 19 1970
LIBRARY &
DOCUMENTS SE...

THE CLIMB OF FRANK LOOPS IN F.C.C. METALS OF LOW STACKING FAULT ENERGY PART I. NUCLEATION OF CLIMB; THE PROCESS OF TETRAHEDRA COLLAPSE

B. Escaig

December 1969

AEC Contract No. W-7405-eng-48

TWO-WEEK LOAN COPY

This is a Library Circulating Copy which may be borrowed for two weeks. For a personal retention copy, call Tech. Info. Division, Ext. 5545

LAWRENCE RADIATION LABORATORY
UNIVERSITY of CALIFORNIA BERKELEY

UCRL-19117

DISCLAIMER

This document was prepared as an account of work sponsored by the United States Government. While this document is believed to contain correct information, neither the United States Government nor any agency thereof, nor the Regents of the University of California, nor any of their employees, makes any warranty, express or implied, or assumes any legal responsibility for the accuracy, completeness, or usefulness of any information, apparatus, product, or process disclosed, or represents that its use would not infringe privately owned rights. Reference herein to any specific commercial product, process, or service by its trade name, trademark, manufacturer, or otherwise, does not necessarily constitute or imply its endorsement, recommendation, or favoring by the United States Government or any agency thereof, or the Regents of the University of California. The views and opinions of authors expressed herein do not necessarily state or reflect those of the United States Government or any agency thereof or the Regents of the University of California.

THE CLIMB OF FRANK LOOPS IN F.C.C. METALS OF LOW STACKING FAULT ENERGY*

PART I. NUCLEATION OF CLIMB; THE PROCESS OF TETRAHEDRA COLLAPSE

B. Escaig†

Inorganic Materials Research Division, Lawrence Radiation Laboratory,
Department of Materials Science and Engineering, College of Engineering,
University of California, Berkeley, California

December 1969

---

*This work done under the auspices of the U. S. Atomic Energy Commission.

†Now in Laboratoire de Physique des Solides associe au C.N.R.S.
91 - Orsay, France

The climb mechanism for dissociated dislocations may be strongly dependent on such conditions as the point defect concentration and the stacking fault energy. Experimentally, the direct way of studying such a climb is to observe, after a convenient hard quench, the growth and the shrinkage of those dislocations which are produced in order to eliminate the excess vacancies. In many f.c.c. metals of medium or low stacking fault energy, these dislocations are found to be either stacking fault tetrahedra or Frank loops, i.e. a prismatic 1/3<111> imperfect dislocation loop bounding a faulted region of a (111) plane. Two different climb processes can be investigated:

(1) during the ageing following the quench, loops grow by climb in the presence of a high supersaturation of vacancies. Climbing should then take place by locally shifting the stacking fault, a dipole of imperfect dislocations, or jog line, being formed along the edge of the shifted region.[1] This mechanism requires a strong thermodynamic driving force and is expected to operate only for low stacking fault energy and high point defect supersaturation. Clarebrough and Morton showed recently[2] clear experimental evidence for this mechanism in quenched silver, and some copper-aluminum alloys.

(2) An entirely different process should occur during subsequent annealing at temperature high enough to observe the shrinkage of these loops. Climb then occurs under nearly equilibrium vacancy concentration throughout the crystal.[3] Ledges, jog lines or imperfect dipoles are unable to develop, so the preceding climb mechanism must be ruled out; instead climb probably takes place through jog diffusion.

The purpose of the following is to study this last climbing process in relation to the annealing out of Frank loops in low stacking fault energy metals. In these metals, dissociation of Frank loops makes their annealing more difficult. It is easy to show that a Frank dislocation should dissociate into a Shockley and a stair rod dislocation, the dissociation width being, for the infinite straight Frank dislocation:

$$d_o = \frac{\alpha}{\gamma}, \quad \alpha = \frac{\mu b^2}{18\pi k}, \qquad k = 1 - \nu \qquad (1)$$

where γ is the stacking fault energy, b the smallest lattice period, μ and ν the shear and Poisson modulus. Reasonable values of γ[4] yield appreciable width in metals such as gold, $d_o \simeq 5b$ ($\gamma \simeq 50$ ergs/cm^2) or silver, $d_o \simeq 15b$ ($\gamma \simeq 18$ ergs/cm^2). As a result Frank loops are formed in polygonal shapes, for example, as truncated stacking fault tetrahedra, with the initial (111) fault boundaries along the three <110> stair rod directions of that plane and with faulted ribbons on the three other {111} planes. In order to cause such a truncated tetrahedra to climb or shrink, an energy barrier has to be overcome; the short stair rod segment formed at a corner has first to be dissociated into two attractive shockleys, resulting finally in the formation of a short length of a new 120°-edge on the loop (fig. 1). This climb nucleation process is described in Part I, while Part II of the paper deals with the resulting steady state climb and the corresponding annealing kinetics.

The nucleation step needed to start climb consists in the evaporation of a few vacancies from loop corners, resulting in a critical blunting of corners of the intitial truncated tetrahedron. Following the usual nucleation theory, the activation energy should be the sum

of the self diffusion energy and the top energy of the barrier to be overcome. This energy barrier is strongly dependent on the stacking fault energy. It is found to be negligible for stacking fault energy γ larger than $4.\ 10^{-3}$ μb, i.e. a dissociation width smaller than 7b, while increasing rapidly for lower stacking fault energy. Values as high as 3 or 4 eV are reached for $\gamma \simeq 2.10^{-3} \mu b$. Accordingly Frank loops in gold should shrink as soon as self diffusion becomes active; any loop stability at higher temperature, as observed erratically, (5)-(7) should be due to impurity pinning. In contrast, for silver, the activation energy is computed to be 5 or 6 eV, i.e. there should be no observable loop shrinkage, even at temperature as high as 1000°C.

However, loops have sometimes been observed to shrink in silver[6] at about 600°C. To explain these observations, a modification to the usual nucleation theory has recently been proposed by the author. It is shown that for some cases, including loop shrinkage, the rate controlling activation energy might be given not by the top energy, but by an energy associated with some of the initial steps up the energy barrier. This can be true if configurations are periodically reached far below the top of the energy barrier for which the backward process, going down the hill, is much harder than the forward process, going up the hill. This modified nucleation theory can explain loop shrinkage in silver and alloys of low stacking fault energy.

Finally, it is suggested that tetrahedra should collapse to Frank loops much more easily than usually assumed.[9] The energy barrier is

very similar to that for initiation of shrinkage of a triangular Frank loop. As a result, while almost no barrier is expected in the case of gold, it increases up to about 20 eV for silver. However, the modified nucleation theory predicts possible tetrahedra collapse even for silver. Similarly impurities can pin the tetrahedra corners very strongly, explaining erratic observed behavior. The direct observations of Yokota and Washburn fully support this collapse model in gold. In low stacking fault metals, further experimental observations are needed for testing the modified nucleation theory.

In the following, we explain first our climb model, then we give numerical results, beginning with the energy barrier obtained for loop shrinkage; tetrahedra collapse is then discussed a little more extensively. The nucleation theory is finally presented, before comparing with experimental data.

Throughout the derivations, we use the standard linear, isotropic elastic theory; however, for core-like problems associated with elementary jogs on dislocation lines it is realized by the author that only a semi-quantitative approach can be claimed.

1. Climb Model

Direct electron microscope observations show polygonal Frank loops climbing much more consistently at 120° corners than at 60° corners (see ref. (5) for copper and (7) for gold). Yokota and Washburn related the higher climb efficiency of 120° corners to the dissociation of Frank loops (fig. 1). It is seen immediately that easier jog nucleation should occur at those corners where dislocations are necessarily constricted, as opposed to 60° corners where short stair rod segments form to stabilize the loop. Following Yokota and Washburn, we assume that

climb by jog nucleation and diffusion can only start at those 60° corners where new 120° edges are formed. In Part I of the paper, we are concerned with the nucleation of such a new 120° edge on a triangular Frank loop. The climbing process itself is studied in Part II, i.e. the activation energy for steady state climb, and the growth of these newly formed 120° edges.

To study the nucleation of stable 120° edges, the model pictured in fig. 2 is considered. Thomson tetrahedron notations are used. A stair rod segment is split at a corner following the reaction $\delta\gamma \rightarrow B\gamma + \delta B$, resulting in a short new 120° Frank segment PQ and two attractive Shockleys PR, RQ. Since the total loop area is reduced, this dislocation structure requires the evaporation of a few vacancies from the corner, and is equivalent to the non-conservative motion of the Frank segment PQ. Two simplifications are introduced. Because the critical length PQ we found was always small, of the order of the normal dissociation width d_o, we consider PQ as an undissociated Frank dislocation. Also, the Shockleys PR, RQ are assumed to be straight segments, so that it is possible to compute the total loop energy for any given triangle PQR as the sum of interaction energies between two straight dislocation segments, the expression for which is well known.[4]

We carried out calculations with a CDC 6600 computer. Details of the computation are given in the Appendix. The triangle PQR is defined by two parameters, the length PQ and the angle (RO, RQ). For a fixed length PQ, the point R is first chosen along the edge OR so as to minimize the total energy. This minimum energy is then plotted versus the length PQ to show how the loop energy varies during shrinkage.

The general shape of the curve is easy to explain. At large values of PQ, the loop energy decreases for increasing PQ due to the reduction of total dislocation line length. For small PQ, this reduction in line energy is balanced by an energy increase due to the dissociation of the stair rod into two attractive Shockleys at the loop corner. If this stair rod is long enough, or the stacking fault energy low enough, the dissociation term may prevail in the total energy, resulting in an initial increase in the energy versus PQ diagram, followed by a uniform decrease, i.e. an energy barrier configuration (fig. 3). Numerical values of this barrier are discussed below for the shrinkage of Frank loops followed by the application to tetrahedra collapse.

2. Frank Loop Shrinkage

Figure 3 shows numerical results obtained for Frank loop shrinkage in gold as an illustrative example. The energy barrier for nucleating a new 120° edge from a sharp 60° corner behaves differently, depending on the stacking fault energy:

(i) No energy barrier is found for stacking fault energies larger or equal to 4.10^{-3} μb ($d_o \leq$ 7b). This result depends only slightly on loop size and on elastic constants, so it still holds approximately for other f.c.c. metals. In such cases Frank loops should shrink continuously provided only that the necessary thermal energy is available for self diffusion (curves A and B, fig. 3).

(ii) Even for lower stacking fault energy metals sharp 60° corners are never stable (curve C, fig. 3). We found invariably that blunting a corner by an amount PQ = 2.5b (i.e. evaporating three vacancies from the corner) stabilizes the loop by about 1 eV. Although continuum elastic theory is questionable for such short edges, it

seems reasonable to expect some rounding of corners from line energy considerations. A blunted corner configuration also provides sites for impurity atoms which might strongly pin the loop corner.

(iii) The energy barrier† increases rapidly with decreasing stacking fault energy (fig. 4); also some size dependence is found. Larger loops have less widely dissociated edges, so have smaller barriers. Critical lengths PQ are of the order of the dissociation width, fig. 5, and correspond to evaporating a few tens of vacancies. Finally critical triangles PQR are found to be almost perpendicular to the loop plane, with a ratio PR/PQ ≃ 1.35, and the apex R at approximately the center of the original 60° corner stair rod.

3. Tetrahedra Collapse and Shrinkage

Nucleation of tetrahedra collapse is thought to be the same process as nucleation of a new edge on a Frank loop. The shrinkage of tetrahedra has been alternatively described in the literature[10, 11] by vacancy emission through propagation of jog lines across tetrahedron faces. However, such jog lines can grow only under a strong super or undersaturation of point defects;[1, 11] this last mechanism should not apply under annealing conditions. Tetrahedra collapse is usually treated as a glide mechanism, which is the reverse of the formation process.[9, 12] In order to compare the model suggested here with this conservative collapse process, we first need to refine the conservative collapse model, then we develop our non-conservative model.

---

†This energy barrier is computed as the energy difference between the maximum and the minimum shown on curve C, fig. 3.

3.1 Conservative Tetrahedra Collapse

Collapse by the reverse formation process assumes a symmetrical, equilateral triangle of Shockley dislocations sweeping down the tetrahedron faces.[9, 12] Successive configurations thus described are not in equilibrium, so do not correspond to a minimum energy path. Therefore we have recomputed this model, allowing the Shockley triangle MNO to rotate around one of its sides into a minimum energy position (fig.6 b). The energy barrier separating the tetrahedron from the dissociated Frank loop is thus found to be about 15% to 20% smaller (fig. 7). In contrast with assigning a constant value to ψ, the inclination angle of the triangle MNO, as is usually assumed ($\psi = 60°$ in ref. (9) and (12),) we allowed a continuous variation of ψ during the collapse, from $\psi = 120°$ for an almost complete tetrahedron ($x \leq 1$, OB = 0) to ψ 60° for a dissociated Frank loop ($x \ll 1$, OB = BM = BN), ψ being about 90°-100° at the critical position in between. Another result is that the stability diagram of Frank loops versus tetrahedra shows a notably reduced domain of metastable Frank loops (domain (b) fig. 9). Therefore, in measuring the stacking fault energy by the method of Loretto et al.[13] -- from largest tetrahedra or smallest Frank triangle left behind moving dislocations after plastic deformation -- it seems reasonable† to take the stability boundary (full curve, fig. 9) as delimiting the range of Frank loop from the one of tetrahedra. That last curve is obviously independent of model (6.a) or (6.b) so the full curve (fig. 9) is the same as the one given by Humble et al.(curve n = 1, fig. 3. ref. (12).

---

†The largest uncertainty in that method is the actual nature of the defect first formed in the process, i.e. a Frank loop, or some intermediate between a Frank loop and a tetrahedron. Therefore, the energy barrier between the two defects should not be of importance.[12, 14]

3.2 Non-conservative tetrahedra collapse

When temperature is high enough for self diffusion to occur there is a much easier way for a tetrahedron to collapse. Curve B, fig. 10, shows an example of a tetrahedron which cannot collapse, fig. 7, by conservative motion, although it is unstable by non-conservative motion, assuming the same size and the same stacking fault energy in both cases. The non-conservative process on which curve B of fig. 10 is based, occurs as does the shrinkage process explained for Frank loops in paragraph 1 and fig. 2(b), where now the triangle MNO is supposed to be shrunk into the tetrahedron apex B. That is to say, some vacancies are evaporated until a critical 120° edge PQ is reached, beyond which the total energy decreases uniformly with increasing PQ, the tetrahedron losing little by little its vacancies. The critical length is small, of the order of 2 to 3 d_o (fig. 5), so it would not be visible under the electron microscope.

Whether or not a collapse into a Frank loop occurs after passing this energy hump depends on the relative stability of the Frank loop and the tetrahedron. If small enough (region (c) fig. 9), a tetrahedron can never collapse to a Frank loop; rather the 120° edge PQ goes on growing (see for example fig. 10, curve B) until its attraction with the stair rod (CD, Bα) prevails, resulting in the Shockley triangle (BCD, Bα) which disappears immediately by glide. On the contrary, if the Frank loop is actually a lower energy configuration (region (a) fig. 9), the tetrahedron should collapse when the edge PQ is long enough to allow for glide rearrangement. The loop produced has the same blunted corner as the parent tetrahedron, so it should go on evaporating its vacancies. (for proof see fig. 5).

The energy barrier (computed as the difference between the maximum and the minimum energy) shown as curve A, fig. 10 is very similar to that

found for loops. No barrier is found for stacking fault energies larger or equal to 7.10^{-3} μb ($d_o \leq 5b$). Again, even for lower fault energies, sharp 60° corners are not stable; rather, tetrahedron corners should be blunted by the same amount as for loops: evaporating three vacancies from a sharp corner (PQ = 2.5b) always stabilizes the tetrahedron by about 1 eV (curve A, fig. 10). Finally the energy barrier is low for gold or copper (smaller than 1 eV), but increases rapidly with decreasing fault energy (fig. 8), up to 4.5 $\mu b^3 \simeq$ 23eV for silver ($d_o \simeq 15b$). Accordingly, as long as the maximum energy of the barrier is considered, tetrahedra collapse by this mechanism remains difficult for low fault energy metals, although being quite efficient for intermediate fault energy metals. However, we show in the next section that the rate controlling energy should not always be considered to be the maximum energy of the barrier.

4. A Modified Nucleation Theory

This modification to the usual nucleation theory has recently been proposed by the author;[8] a brief account is given here, taking as an example the Frank loop shrinkage.

Let us first consider how the usual nucleation theory[15] describes the building up of a new 120° edge on a Frank loop. In order to reach the critical 120° edge, which has the maximum energy, vacancies have to be evaporated one by one, through a series of bimolecular equilibrium reactions:

$$\begin{array}{l} \cdots\cdots\cdots\cdots\cdots\cdots \\ \alpha + (i-1) \rightleftarrows i \\ \alpha + i \rightleftarrows i+1 \\ \cdots\cdots\cdots\cdots\cdots\cdots \end{array} \qquad (2)$$

where α is an atom of the metal and i is the triangle shaped cluster

of i atoms which already fills in the loop corner. Any i-sized cluster is thus growing both by a forward reaction, $\alpha + (i - 1) \rightarrow i$, which is assumed to be slow since it is going up the hill, and by a backward reaction, $i + 1 \rightarrow \alpha + i$, which is considered to be fast since it brings the system to a lower energy state. Solving the whole set of such equilibriums for steady state conditions yields a rate of nucleation depending only on the top energy of the barrier through an Arrhenius type law.[16]

We would point out, however, that for certain types of cluster j, the backward reaction $j \rightarrow j - 1$ may practically never occur because the forward reaction $j \rightarrow j + 1$ is so much easier. Consider for example the simple case where a length PQ = (n + 0.5) b is left free of jogs (fig. 11), after evaporating a number $j = 0.5n(n + 1)$ vacancies (where n is an integer) from a loop corner. To evaporate or condense other vacancies, a jog must then be nucleated at the corner P, and propagated by diffusion along PQ. It is easy to see that evaporating a vacancy (forward reaction $j \rightarrow j + 1$) requires a much easier jog nucleation (nucleation type (1)) than condensing a vacancy (backward reaction, $j \rightarrow j - 1$; nucleation type (2)). Such a jog difference has been invoked[3] to explain, in high stacking fault energy metals, why prismatic loops grow in a polygonal shape (involving the type 2 of jog nucleation) and shrink in a round shape (type 1). Even a rough estimation, using the standard elastic theory and following the procedure given in the appendix† yields an energy difference between jog (2) and

---

†ΔU should not be very dependent on the dissociated structure of the Frank loop. Accordingly, ΔU is computed here for an undissociated triangular Frank loop (fig. 11). ΔU is obtained numerically, in computing all the self and elastic interaction terms of loop segments, for PQ = 5.5b and a loop size CD = 300b. ΔU decreases slightly with increasing PQ, reaching the two thirds of that value when PQ is very large (PQ = 150b).

jog (1) of about $\Delta U \simeq (\mu b^3/18\pi K)(1.5 + \sqrt{3}\, b/d_o) \simeq .25$ eV for silver or gold. At an annealing temperature of 400°C ($kT \simeq 0.056$ eV), this means that, once an edge PQ is completed, there is a thermal probability about $\exp(\Delta U/kT) \simeq 100$ times higher for going forward than for going backward. That is to say, the edge PQ can practically only grow, the reaction leading to a shorter edge being so much more difficult to start. In a way, this mechanism is similar in operation to some car-jacks: periodically a blocking device prevents the lifted car from going down again.

The kinetics of the process is easily obtained. Instead of the preceding series of equilibrium reactions, see equ. (2), we can summarize the whole process through a set of <u>chain</u> reactions:

$$\begin{array}{l} 1 + 2\alpha \rightarrow 2 \\ \cdots\cdots\cdots\cdots \\ n + (n+1)\alpha \rightarrow n + 1 \\ \cdots\cdots\cdots\cdots \\ n^* + (n^*+1)\alpha \rightarrow n^* + 1 \end{array} \qquad (3)$$

describing the building of an edge $(n + 1)b$ long from the parent edge, nb long, until the critical size n^* is reached. The rate of the nth reaction is expressed as $v_n = k_n[n]$, where k_n is the rate constant and $[n]$ the concentration of n-sized edges. Assuming a thermal equilibrium between all the $n + 1$ intermediate steps leading from an n-edge to an $(n + 1)$ edge, similar to equ. (2), yields:[16]

$$k_n \simeq \exp -[(\Delta G_n + U_D)/kT], \quad \Delta G_n = G(n + 1) - G(n)$$

U_D being the self diffusion energy, and $G(n)$ the energy of an n-sized edge PQ, shown for example curve C, fig. 3. Finally, to assure no accumulation in any reaction products, all reaction rates in (3) must be equal, under steady state conditions, so:

$$v = k_1[1] = \ldots = k_n[n] = \ldots = k_{n*}[n*]$$

This means that a higher step ΔG_n, or a lower k_n induces an accumulation of nuclei n, or a higher [n] until compensation takes place so that the product $k_n \cdot [n]$ is kept constant. The rate of the whole process should thus be:

$$v \sim [1] \exp - [(\Delta G_1 + U_D)/kT] \qquad (4)$$

where [1] is the initial concentration of loops and $\Delta G_1 = G(2) - G(1)$ the height of the first step.

In a more realistic approximation, it is hard to rule out completely the possibility of reverse reactions on the very first steps of equ. (3), because the loop dissociation was neglected in evaluating ΔU. For n = 2, 3, or 4 it would be necessary to evaluate how much energy is gained in recombining the attractive Shockleys into stair rods. As a result, if yb is the longest edge length for which reverse reaction occurs, the final reaction rate should be given instead of equ. (4) by:

$$v \sim [1] \exp - [(G(y + 1) + U_D)/kT] \qquad (5)$$

However, the maximum energy configuration is reached at a stage far beyond these first few steps, at least for the case of low stacking fault energy metals (see fig. 5); therefore the rate controlling energy, G(y + 1) is expected to be <u>much less</u> than the maximum energy G(n*). Fig. 12(a) and (b) give these energies G(y + 1) for y + 1 = 3, 4, or 5. Assuming for example y = 4, it seems that the rate controlling energy for loop shrinkage or tetrahedron collapse, in silver, should be only U_D + 0.8eV $\simeq$ 2.7eV.

5. Experimental Comparison and Discussion

We discuss first the case of gold, in which Yokota and Washburn[7] quantitatively investigated the annealing behavior of quench defects by

transmission electron microscopy. Then we consider briefly the case of silver, a low fault energy metal.

Bulk specimens of gold were quenched by Yokota and Washburn from 1000°C into an ice water bath, and aged for several hours at a temperature of 150°C. Then thin foils were cut from specimens, and heated outside the microscope at a fixed annealing temperature. During the loops shrinkage, the specimen was periodically cooled and returned to the micrsocope to record loop size. Because they observed no influence of the distance to the foil surface, either on the shrinkage rate or on the climb nucleation, it seems reasonable to neglect image effects due to surfaces, and to apply the preceding computations, strictly valid only in the bulk.

A central parameter is obviously the stacking fault energy. For gold, it has been measured by the method of Loretto et. al.[13] from the largest tetrahedron or the smallest Frank loop found after plastic deformation. From the diagram of fig. 9, and taking as criterion the stability boundary, a value of $\gamma \simeq 50$ ergs/cm^2 and $d_o \simeq 5$ or 6b is thus obtained. However, because the critical size observed is of the order of 200Å, i.e. near the limit of resolution, these figures should be taken with at least an error range of ± 30%.

For such a fault energy, Frank loops should shrink as soon as self diffusion becomes active. Experimental observations show that some loops do shrink without delay: see fig.2, ref. 7(a), or fig. 4 ref. 7(b) loops no. 13, 15, just below no. 10, beside no. 3, etc... But many other loops do not shrink at all, even during ten hours, or shrink

somewhat erratically with a delay of some hours. Such examples suggest a strong impurity pinning. We have shown that the actual corner structure of a dissociated Frank loop is blunted. Impurity atoms should diffuse toward corners during the ageing, and should be able to pin a corner, preventing a new 120° edge from being nucleated. The same pinning effect probably causes some loops to shrink asymmetrically, only one apex being active. Such an impurity effect has already been suggested by Washburn and Yokota.[7b]

The most important observation on tetrahedra is that numerous tetrahedra do collapse into Frank loops during the annealing. The set of micrographs of fig. 2, ref. 7(a), or fig. 4, ref. 7(b), shows that 40% of tetrahedra have collapsed during ten hours of annealing at 300°C. Surface effects should not be involved, since they do not affect the observed shrinkage rate. Also, local heating under the electron beam should be discarded since neighboring defects are often not affected. These experimental observations are not explained by the previous theories[4, 9, 12] which predict a huge energy hump between the tetrahedron and the Frank loop. Our non-conservative model for tetrahedra collapse (§3.2) can account for these observations. For a dissociation width d_o between 5 and 6b, fig. 8 gives an energy barrier $u \simeq 0.05\ \mu b^3 \simeq 0.25$ eV; even for larger dissociation, fig. 12(b), it still yields a rate controlling energy of about the same value. The collapse frequency for a four apexes tetrahedron should then be $\nu \simeq 4\nu_D \exp\,[-(U_D + u)/kT]$, ν_D being an atomic frequency. With $\nu_D \simeq 10^{13}\ \mathrm{sec}^{-1}$, $U_D + u \simeq 2.05$ eV $T = 300°C$ one has $\nu \simeq 10^{-4}\ \mathrm{sec}^{-1}$, giving a reasonable probability of collapse after one hour of annealing. The fact that many tetrahedra still remain after

ten hours of annealing is evidence that an impurity pinning very similar to the loop pinning occurs also for tetrahedra. It is observed that when a tetrahedron collapses into a Frank loop, this loop almost always starts shrinking immediately, as predicted (see tetrahedra no. 17, 18, and the one beside loop no. 9, ref. (7)). However, impurity pinning could introduce delays at any stage under certain conditions.

Finally, tetrahedra shrinkage has usually been considered to be more difficult than we suggest here. For example, Meshii and Kauffman gave an activation energy of 4.7 eV on the basis of electrical resistivity measurements. It is suggested that this value might correspond rather to an unpinning from impurities.

It will be very useful to test the predictions of this model with experimental observations on a low stacking fault energy metal such as silver. In particular the simple occurance in silver at 500°C or 600°C of the collapse of tetrahedra, or the shrinkage of Frank loops would confirm the modified nucleation theory proposed here. Already some isolated examples of such loop shrinkage have been reported in silver, at temperature of 620°C by Smallman et al.[6]

SUMMARY

A model is suggested for the shrinking under annealing conditions of triangular Frank loops, when dissociated into truncated tetrahedra, and of stacking fault tetrahedra. The process starts with evaporation of a few vacancies from a sharp 60° corner, resulting in nucleating on the defect a short length of 120° edge. Once a critical blunting of the corner is reached, the defect goes on shrinking, decreasing its energy and losing little by little its vacancies. It is shown that tetrahedra should collapse while shrinking. For pure metals of intermediate stacking fault energy, like gold or copper, loops or tetrahedra should start shrinking as soon as self-diffusion is possible. Their stability, as sometimes reported, should be evidence for an impurity pinning effect. Finally a modification of the usual nucleation theory is presented, leading to a shrinkage of these defects at observable rates at temperature 0.5 Tm even in the case of low stacking fault metals such as silver.

ACKNOWLEDGEMENTS

The author is indebted to Professor J. Washburn for reading the manuscript and for many helpful discussions. The support of this work by the United States Atomic Energy Commission, through the Inorganic Materials Research Division of the Lawrence Radiation Laboratory is gratefully acknowledged.

APPENDIX

1) INTERACTION ENERGY FORMULAS

We used the interaction energy formulas, as given by Hirth and Lothe[4] for two straight segments of dislocation. However, the general equation they give in the non coplanar, non parallel case, equ. 6-26 in ref. (4), is not ready to use in a computer. Furthermore, the segment coordinates are related to their common perpendicular. Therefore, we give below the equivalent explicit expression of this interaction. The two dislocation segments are defined through:

$$\underset{\sim}{b}_i,\ \underset{\sim}{S}_i,\ \underset{\sim}{OD}_i, \ell_i \qquad i = 1,2$$

which are respectively, the Burgers vector, the unit line vector, the position vector of the segment origine D_i relative to a fixed origin O, and its length ℓ_i, so that the dislocation segment is $\underset{\sim}{D}_i \underset{\sim}{D}'_i = \ell_i \underset{\sim}{S}_i$, $\ell_i > 0$. Then we introduce the notations†:

$$S = |\underset{\sim}{S}_1 \times \underset{\sim}{S}_2| \ , \quad \underset{\sim}{N} = (\underset{\sim}{S}_1 \times \underset{\sim}{S}_2)/S, \qquad z = (\underset{\sim}{OD}_2 - \underset{\sim}{OD}_1) \cdot \underset{\sim}{N}$$

So the elastic interaction energy is written:

$$W = \frac{\mu}{4\pi} \left[A_1 f_1 + \frac{1}{1-\nu} \{A_2 f_2 + A_3 f_3 + A_4 f_4 + A_5 f_5\} \right]$$

where the numbers A are:

$$A_1 = (\underset{\sim}{b}_1 \cdot \underset{\sim}{S}_1)(\underset{\sim}{b}_2 \cdot \underset{\sim}{S}_2) - 2(\underset{\sim}{b}_1 \times \underset{\sim}{b}_2)(S_1 \times \underset{\sim}{S}_2)$$

$$A_2 = (\underset{\sim}{b}_1 \cdot \underset{\sim}{S}_1 \times \underset{\sim}{N})(\underset{\sim}{b}_2 \cdot \underset{\sim}{S}_2 \times \underset{\sim}{N})$$

$$A_3 = (\underset{\sim}{b}_1 \cdot \underset{\sim}{N})(\underset{\sim}{b}_2 \cdot \underset{\sim}{N})$$

---

†It is to be noticed that in our notations, line 2 is taken as being a distance z above line 1. In the book of Hirth and Lothe,[1] z is defined on the contrary as the distance line 1 is above line 2.

$$A_4 = -(\underset{\sim}{b}_1 \cdot \underset{\sim}{S}_1 \times \underset{\sim}{N})(\underset{\sim}{b}_2 \cdot \underset{\sim}{N})(z/S)$$

$$A_5 = -(\underset{\sim}{b}_1 \cdot \underset{\sim}{N})(\underset{\sim}{b}_2 \cdot \underset{\sim}{S}_2 \times \underset{\sim}{N})(z/S)$$

and the numbers f stand for

$$f_i = f_i(x_2, y_2) + f_i(x_1, y_1) - f_i(x_2, y_1) - f_i(x_1, y_2)$$

the functions $f_i(x,y)$ being defined in Hirth notations (ref. (4), $\theta = (\underset{\sim}{S}_1, \underset{\sim}{S}_2)$) by:

$$f_1(x,y) = I(x,y);\ f_2(x,y) = I(x,y) - z^2\, J(x,y)$$

$$f_3(x,y) = R - \cos\theta(x \operatorname{Log} t + y \operatorname{Log} s)$$

$$f_4(x,y) = \operatorname{Log} t + \cos\theta \operatorname{Log} s;\ f_5(x,y) = \operatorname{Log} s + \cos\theta \operatorname{Log} t.$$

Finally the segment coordinates are computed as

$$x_2 = x_1 + \ell_1 \qquad x_1 = -P + Q\cos\theta \qquad P = (\underset{\sim}{OD}_2 - \underset{\sim}{OD}_1) \cdot \underset{\sim}{S}_1$$

$$y_2 = y_1 + \ell_2 \qquad y_1 = Q \qquad Q = (\underset{\sim}{OD}_2 - \underset{\sim}{OD}_1) \cdot \underset{\sim}{N} \times \underset{\sim}{S}_1 / S$$

2) <u>THE ENERGY FOR BLUNTING A CORNER OF POLYGONAL DISLOCATION DEFECTS</u>

Let us consider a stacking fault tetrahedron, or a triangular Frank loop T. By blunting a corner, as in Fig. 2(b), a part T_1 of the defect is replaced by another part T_1', the rest T_2 remaining unchanged (fig. 2(b): T_1 is the old stair rod "corner" AQ, AR, AP, while T_1 is the Shockley triangle PQR). The blunting energy is then computed as:

$$W = S(T_1') + I(T_1'T_2) - S(T_1) - I(T_1, T_2)$$

where $S(T_1')$ is the total self energy of the isolated defect T_1', and I the interaction energy between T_1' and T_2.

Interaction terms are easily computed as a sum of pair interactions, with expressions given just above. As for the self energy of a segment of Burgers vector b and length L, the corresponding expression is taken as:

$$W_s \propto \operatorname{Log}\left(\frac{2L}{eb}\right)$$

which is equivalent to take a core radius r = b (cf. ref. (4), p. 214).

3) RESULTS AND VERIFICATIONS

Formulas and methods of the preceding sections have been verified by computing the energies of all intermediate configurations between tetrahedron and dissociated Frank loops (fig.6.a), with the same values of parameters as in Jossang and Hirth's paper (ref.(9)): edge length 141b, $\gamma = 2.8\ 10^{-3}$ b, core radius r = b. The result of computation agreed to several digits with Jossang and Hirth's results.

The table below gives as an example the dissociation width of triangular Frank loops. The length MC/b (fig 2 (b)) is given depending on the loop size L = CD, and the normal dissociation width d_o/b (see equ. (1)). Elastic constants of silver are used; those of gold give similar figures, except for some cases for which values in gold case are given between brackets.

d_o/b \ L/b	100	300	500	900	1500	∞
5	8.4(8.2)	6.4	6.1	6.0	5.8	5.78
7	168(159)	9.5(9.4)	8.9(8.8)	8.5	8.3	8.09
9	--	131(129)	118(117)	11.2	10.8	10.40
11		172(169)			13.3	12.71
13		22.2	18.5	16.8	16.0	15.02
15		28.5	22.3	19.8	18.7	17.33
17		37	26.6	22.9	21.5	19.64
19		50.6		26.6	24.5	
21			36.9	29.0		24.27
25			50.6	36.1		28.90

REFERENCES

1. B. Escaig, Acta Met., 11, 595 (1963).
also in J. Friedel, Dislocations, Perg. Press (1964) p. 169.

2. L. M. Clarebrough, A. J. Morton, Int. Conf. on Vacancies and Interstitials in Metals, Julich (1968) p. 200.
Also in Austr. J. Physics, 22, 393, (1969).

3. J. Silcox, M. J. Whelan, Phil Mag. 5, 1 (1960).

4. J. P. Hirth, J. Lothe, Theory of Dislocations, McGraw Hill (1968) p. 764, p. 141.

5. L. M. Clarebrough, P. Humble, M. H. Loretto, Can. J. Phys. 45, 1135 (1967; 1966 Ottawa Conference Proceedings): gold, fig. 11; copper, fig. 6, 10.

6. R. E. Smallman, P. S. Dobson, P. J. Goodhew, Proceedings of the Int. Conf. on the Strength of Metals and Alloys, Tokyo 1967, in Trans. of the Jap. Inst. of Metals, 9, 562 (1968).

7. a. M. J. Yokota, J. Washburn, Phil Mag., 16, 459 (1967);
b. J. Washburn, M. J. Yokota, J. Cryst. Latt. Defects 1 (1969).

8. B. Escaig, J. Cryst. Latt. Defects - to be published.

9. T. Jossang, J. P. Hirth, Phil Mag, 13, 657 (1966).

10. R. Segall, L. M. Clarebrough, M. H. Loretto, Phil Mag. 14, 53 (1966).

11. D. Kuhlmann-Wilsdorf, Acta Met., 13, 257 (1965).

12. P. Humble, R. Segall, A. K. Head, Phil. Mag. 15, 281 (1967).

13. M. H. Loretto, L. M. Clarebrough, R. Segall, Phil. Mag. 11, 459 (1965).

14. P. Humble, C. T. Forwood, Phys. Stat. Sol. 29, 99 (1968).

15. M. Volmer, Kinetic der Phasenbildung, Julius Springer Verlag, Dresden (1939); see D. Turnbull, Solid State Phys., 3, 225 (1956).

16. D. Turnbull and J. C. Fisher, J. Chem. Phys., 17, 1, 71 (1949).

17. M. Meshii, J. M. Kauffman, Phil. Mag., 5, 939 (1960).

TABLE I

	ν	μ (10^{11} dynes/cm^2)	b (A)	μb^3 (eV)	αb (eV)	α/b (ergs/cm^2)	U_D (eV)
Au	0.412	3.10	2.88	4.63	0.136	268.5	1.8
Ag	0.354	3.38	2.89	5.13	0.140	269	1.9

Values for ν and μ are pertinent average, anisotropic moduli, given by Jossang et. al.,[9] αb is defined as $\mu b^3/(18\pi(1-\nu))$. U_D is the self diffusion energy.

FIGURE CAPTIONS

Figure 1. Dislocation configurations at sharp 60° corners A and B, and at 120° corners C and C′

Figure 2. (a) Thomson tetrahedron notations

(b) Dissociated structure of a Frank loop, with a forming 120° edge. The triangle PQR is unfaulted.

(c) Orientation of Burgers vector, line, and extra-half plane for the Frank loop considered as undissociated.

Figure 3. Variation of total loop energy (dislocation and stacking fault) during nucleation of a new 120° edge on a triangular Frank loop, in gold (the initial loop energy is taken as zero energy). x is the shrinkage parameter, $x = 1 - (PQ/L_f)$, and equals unity for a zero 120° edge (original 60° corner). Loop size: $L_f = CD = 300b$. Stacking fault energies in ergs/cm^2: A, $\gamma = 45$ ($d_o = 6b$); B, $\gamma = 38$ ($d_o = 7b$); C, $\gamma = 30$ ($d_o = 9b$). Elastic constants are taken from Table 1.

Figure 4. Energy barrier for nucleating a new 120° edge on a triangular Frank loop, for gold and silver. The energy is plotted versus the dissociation width d_o; values of corresponding stacking fault energies are computed from equ. (1) and Table 1, and are given between brackets. loop size: A, $L_f = 1500b$; B, $L_f = 300b$; C, $L_f = 500b$.

Figure 5. Critical length PQ of the nucleating 120° edge, as a function of dissociation width d_o. Also given are the values of N, the number of vacancies evaporated from the loop corner to build up the new edge PQ, $N \simeq 0.5\ (PQ/b)^2$. Curves A and B

apply to stacking fault tetrahedra (A, silver, tetrahedron size L_t = 300b; B, gold, L_t = 300b). Curves A′ and B′ apply to triangular Frank loops (A′, silver, loop size L_f = 500b; B′, gold, L_f = 300b).

Figure 6. Conservative tetrahedron collapse by glide of a Shockley triangle, down the tetrahedron faces: (a) symmetrical model; (b) equilibrium model; the angle ψ = (ON, OB) is determined so as to minimize the total energy, for a given length MN.

Figure 7. Variation of total energy during a conservative tetrahedron collapse in gold (the tetrahedron energy is taken as zero). x is the collapse parameter, $x = 1 - (MN/L_t)$, and L_t the tetrahedron size, L_t = 70b. Dissociation width d_o = 5b ($\gamma \simeq 6.10^{-3}$ μb ≃ 54 ergs/cm^2). Full curve corresponds to the model of fig. 6, (b). Dotted curve is obtained assuming $\psi = 60°$, fig. 6, (a).

Figure 8. Energy barrier for tetrahedra collapse, versus the dissociation width d_o, related to the stacking fault energy by equ. (1). Full curves are for silver, dotted curves are for gold. Top curves apply to a conservative collapse, bottom curves, to a non-conservative collapse. The magnitude of self-diffusion energy (for gold) to be added to the latter curves is shown for comparison. Tetrahedron size: silver, A: L_t = 1500b; B, L_t = 300b; gold, L_t = 300b.

Figure 9. Stability diagram of dissociated Frank loops versus tetrahedra, depending on the defect edge length, l, and the dissociation width d_o. (The stacking fault energy is given

between brackets for gold or silver). Stability boundary (full curve) and metastability boundary (dotted curve) apply for gold, silver, or copper. "Stability" and "metastability" domains are briefly explained on the schematic energy diagram, shown for a given stacking fault energy as a function of the nature of defect, for different sizes. Critical defect sizes ℓ/b as observed,[13] are indicated for gold, silver, copper (largest tetrahedra or smallest Frank loops).

Figure 10. Variation of total tetrahedron energy during growth of a 120° edge on a tetrahedron, resulting finally in collapsing the tetrahedron. Gold elastic constants are used; curve A applies to a tetrahedron size, L_t = 300b, and a dissociation width d_o = 9b; curve B applies to L_t = 70b, d_o = 5b. Energy is plotted versus the shrinkage parameter $x = 1 - (PQ/L_t)$ corresponding to a 120° edge length PQ (see fig. 2b).

Figure 11. The two kinds of jogs nucleated at corner P; nucleation type (1) is for evaporating a vacancy ($j \rightarrow j + 1$); nucleation type (2) is for condensing a vacancy ($j \rightarrow j - 1$). Schematic.

Figure 12(a). The energy needed to build up on a Frank loop, an extra 120° edge of various lengths nb, versus the dissociation width d_o (or the stacking fault energy, see equ. (1)). Gold, or silver elastic constants are used. Curves A, n = 3; B, n = 4; C, n = 5. Loop size: L_f = 300b (gold) and L_t = 500b (silver). A unit of 0.1 eV is pictured for the gold or silver case.

Figure 12(b). Same as figure 12(a), for a stacking fault tetrahedron. Tetrahedron size: L_t = 300b. A, n = 3; B, n = 4; C, n = 5.

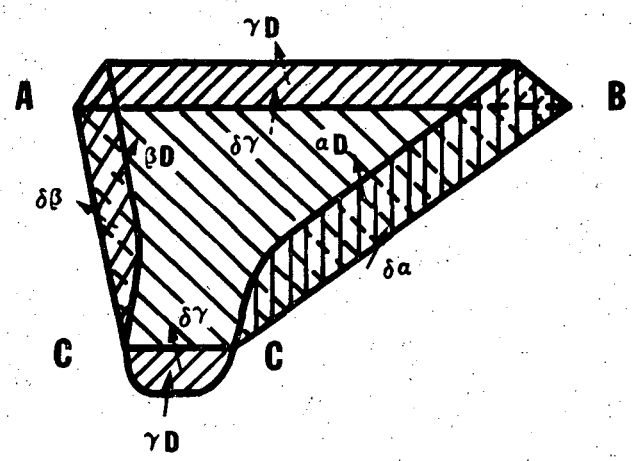

XBL 6912-6650

fig. 1

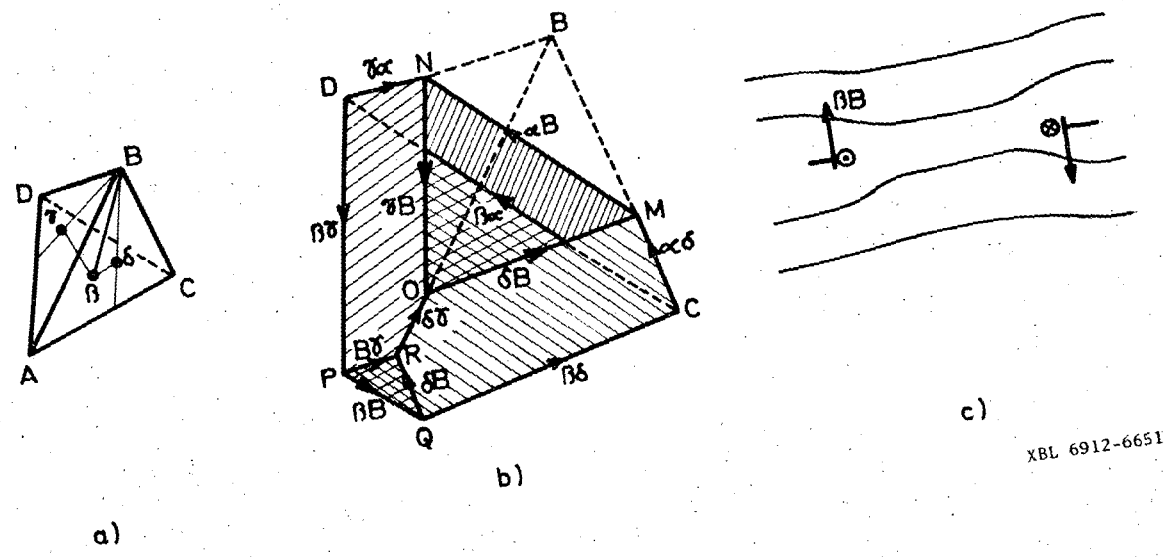

a) b)

fig. 2

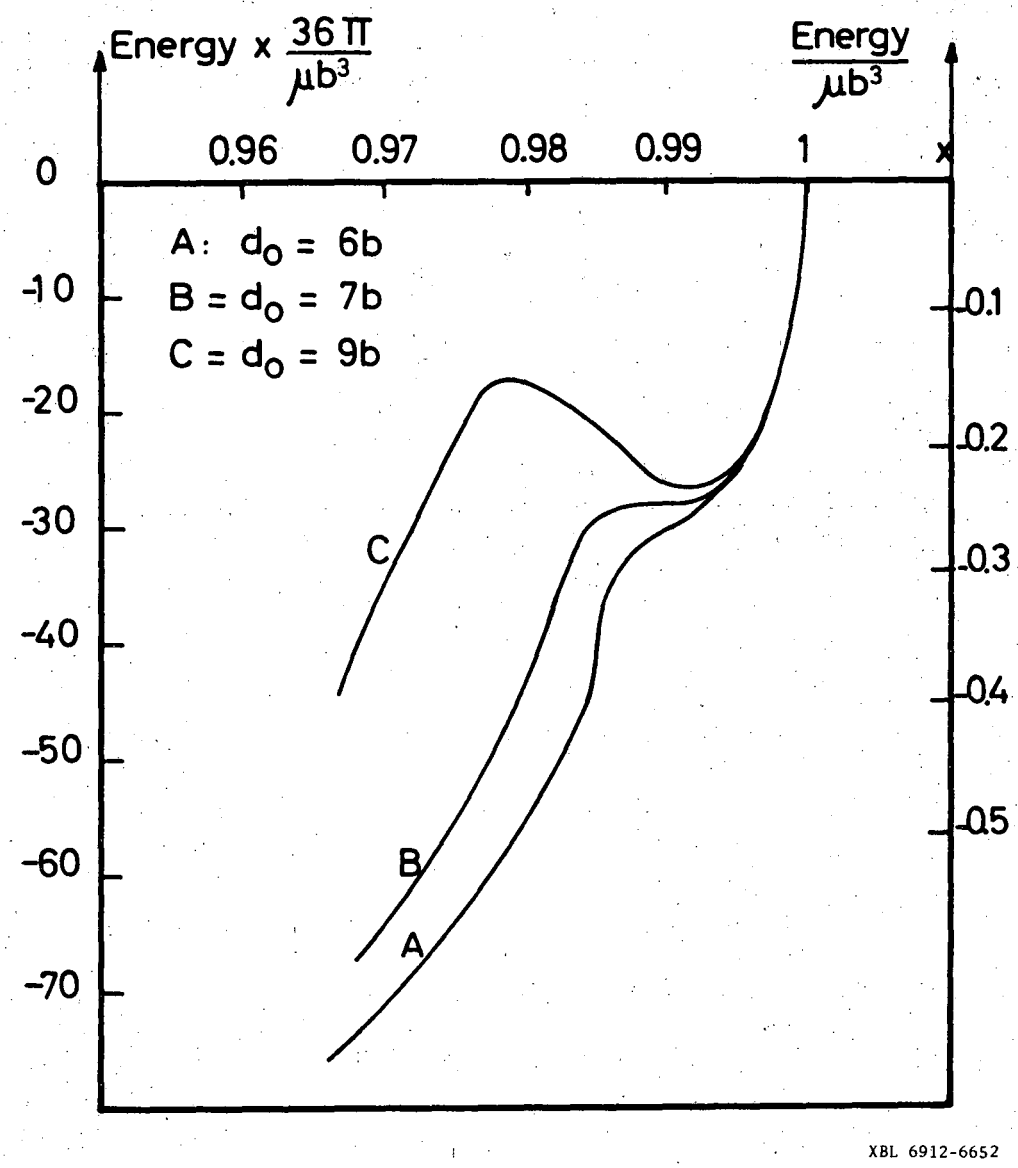
Energy x 36π / μb³
Energy / μb³
0.96
0.97
0.98
0.99
1
x
0
-10
-20
-30
-40
-50
-60
-70
0.1
0.2
0.3
0.4
0.5
A: d₀ = 6b
B = d₀ = 7b
C = d₀ = 9b
C
B
A
XBL 6912-6652

fig. 3

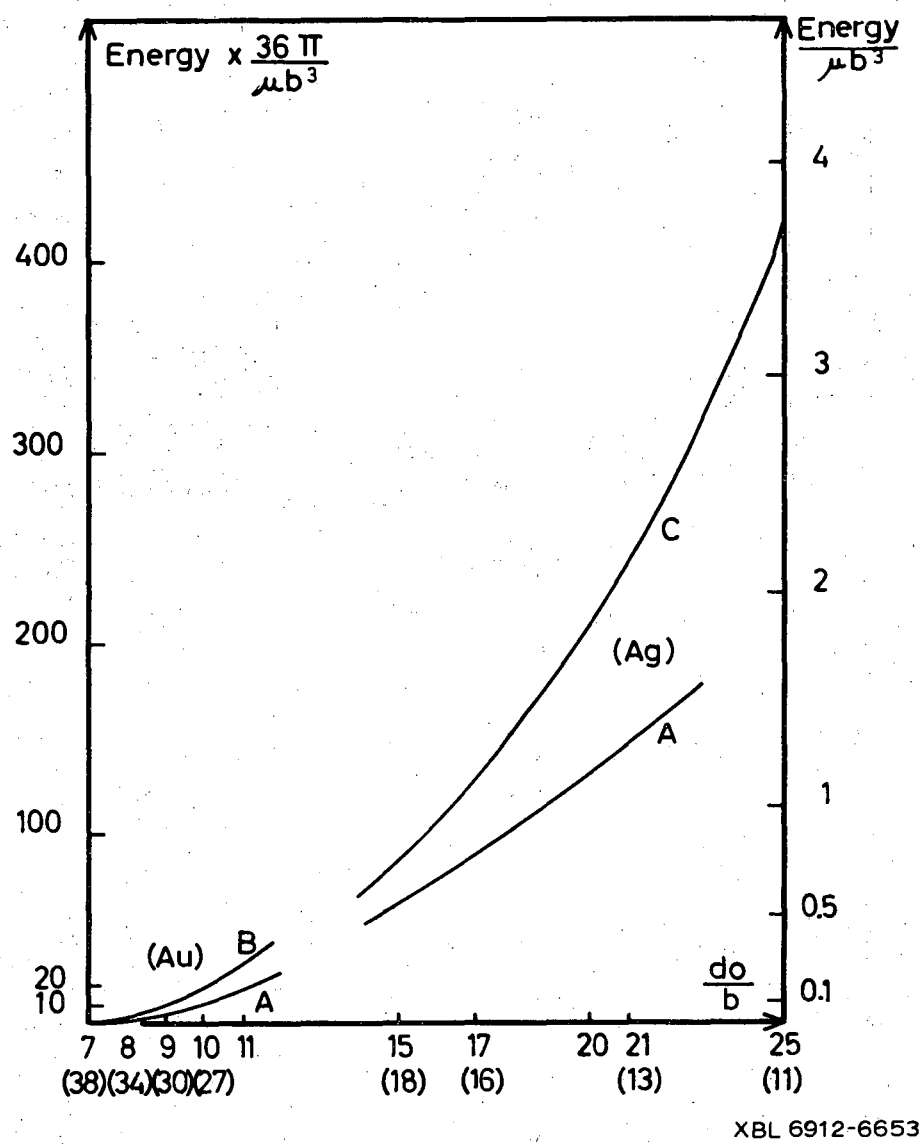
Energy x 36 π / μb³
Energy / μb³
400
300
200
100
20
10
4
3
2
1
0.5
0.1
C
(Ag)
A
(Au)
B
A
do / b
7 8 9 10 11 15 17 20 21 25
(38)(34)(30)(27) (18) (16) (13) (11)
XBL 6912-6653

fig. 4

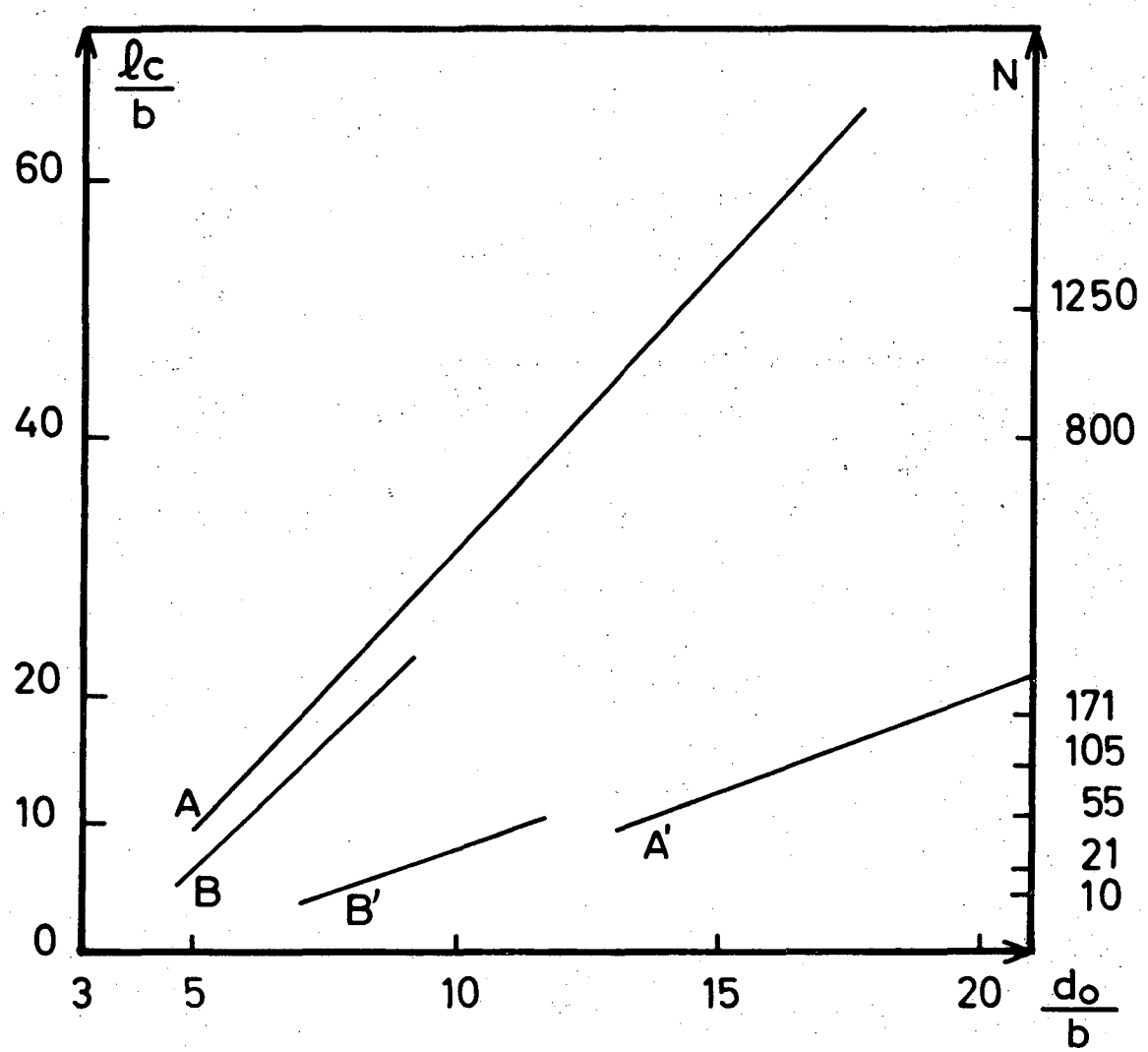

XBL 6912-6654

fig. 5

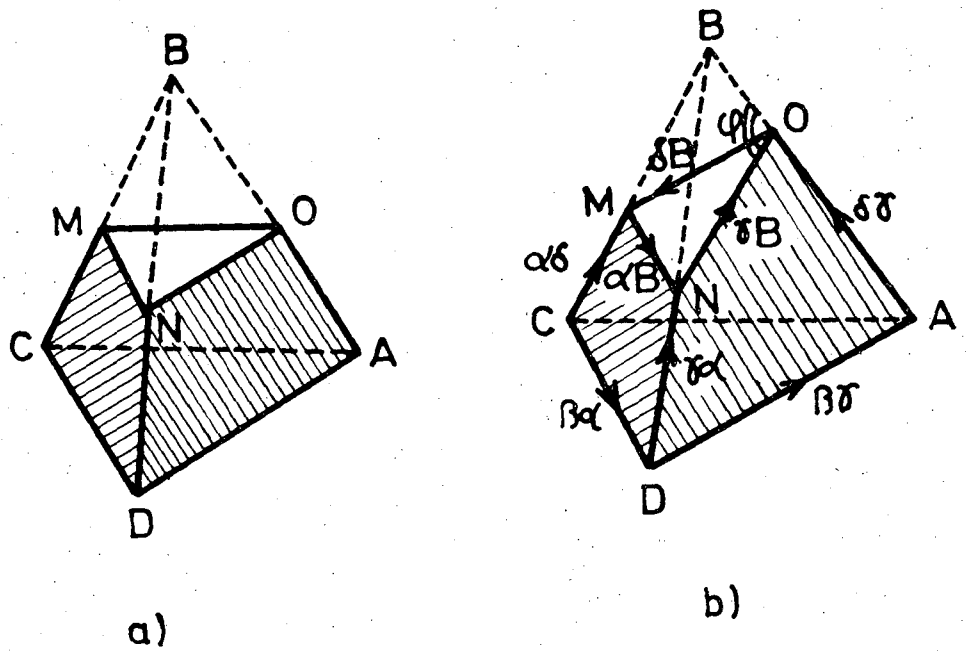

XBL 6912-6655

fig. 6

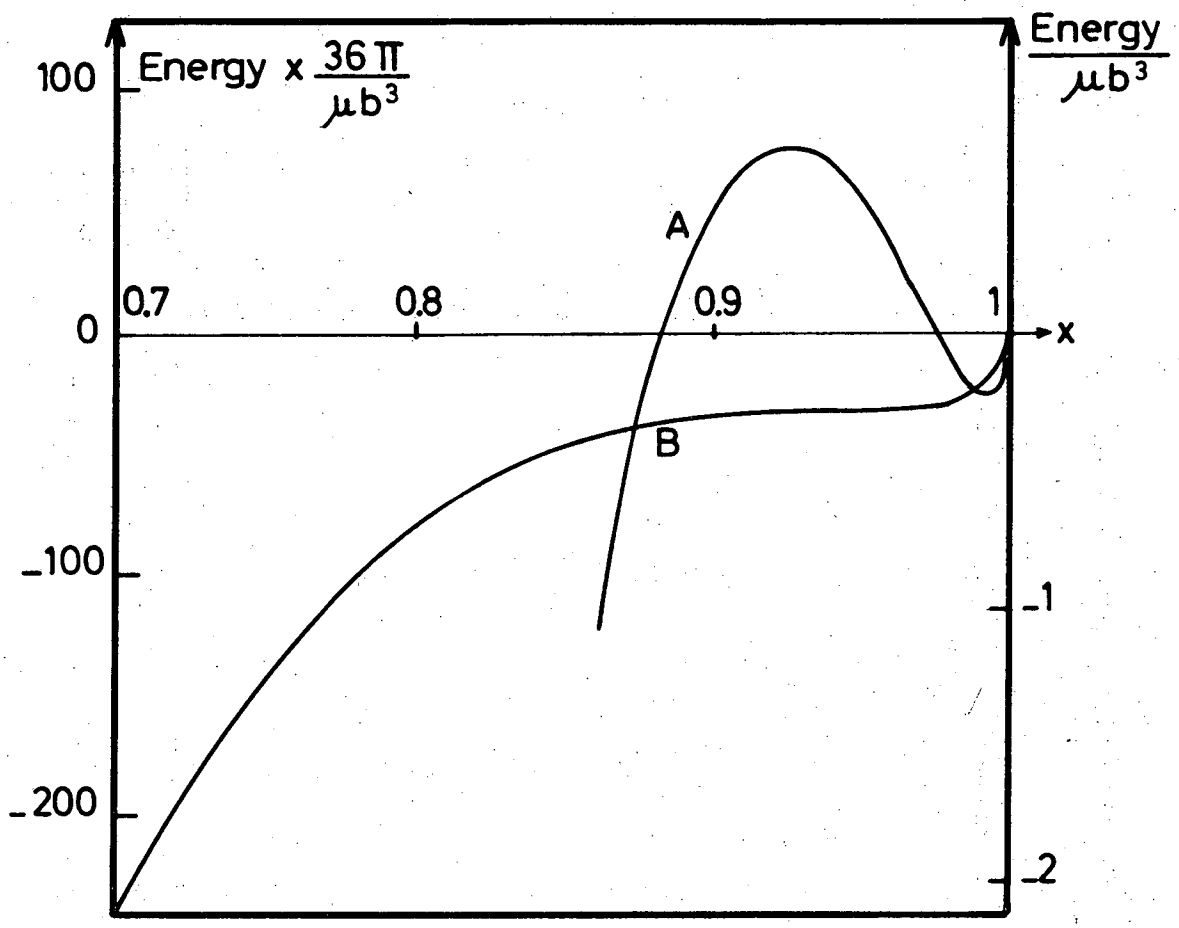

XBL 6912-6656

fig. 7

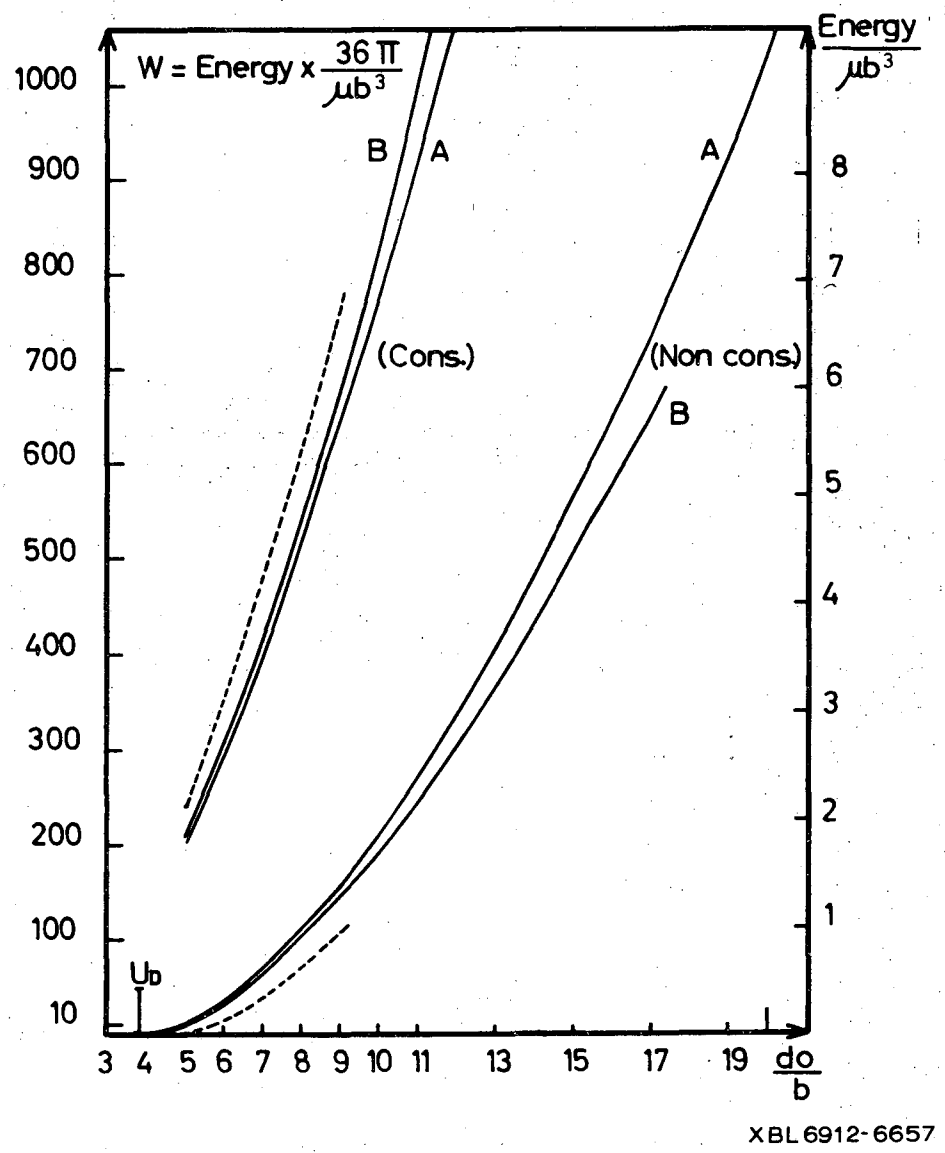
W = Energy x 36 π / μb³
Energy / μb³
1000
900
800
700
600
500
400
300
200
100
10
8
7
6
5
4
3
2
1
B
A
A
(Cons.)
(Non cons.)
B
Ub
3 4 5 6 7 8 9 10 11 13 15 17 19 do/b
XBL6912-6657

fig. 8

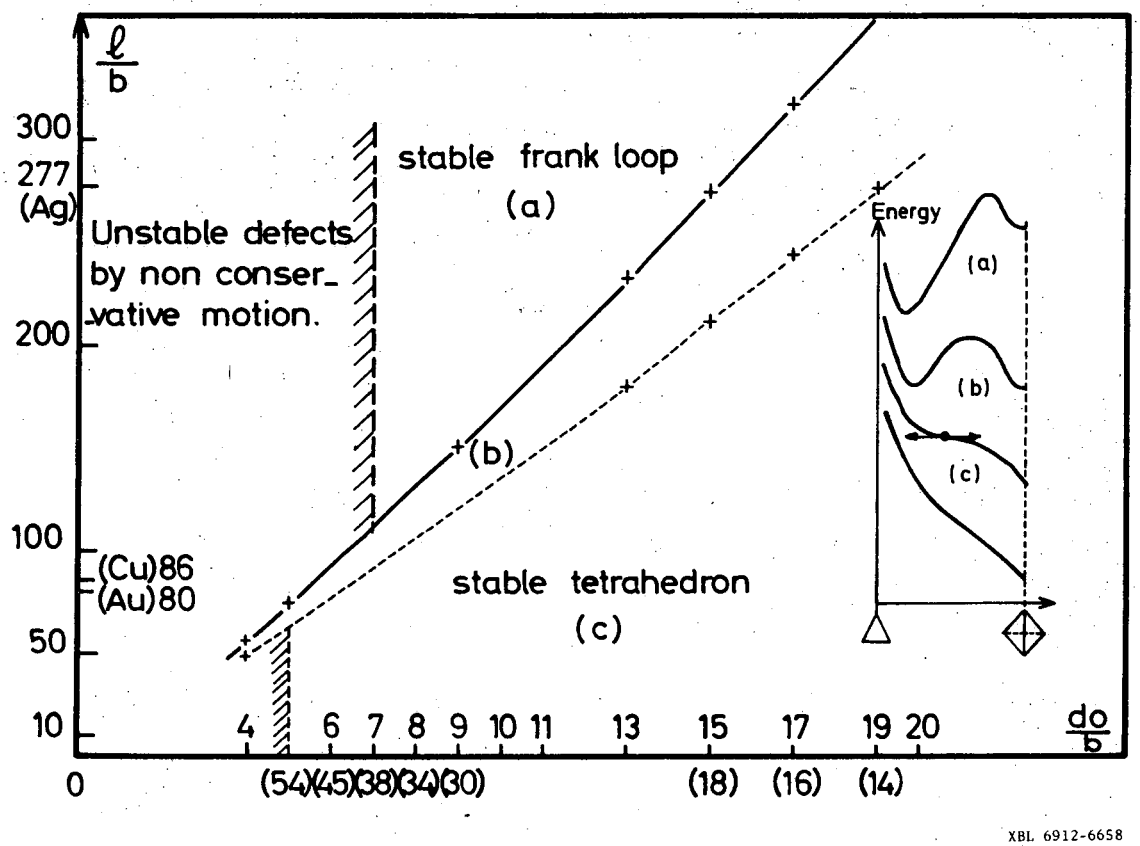
ℓ/b
300
277
(Ag)
200
100
(Cu)86
(Au)80
50
10
0
Unstable defects by non conser- vative motion.
stable frank loop
(a)
(b)
stable tetrahedron
(c)
Energy
(a)
(b)
(c)
4 6 7 8 9 10 11 13 15 17 19 20
do/b
(54)(45)(38)(34)(30) (18) (16) (14)
XBL 6912-6658

fig. 9

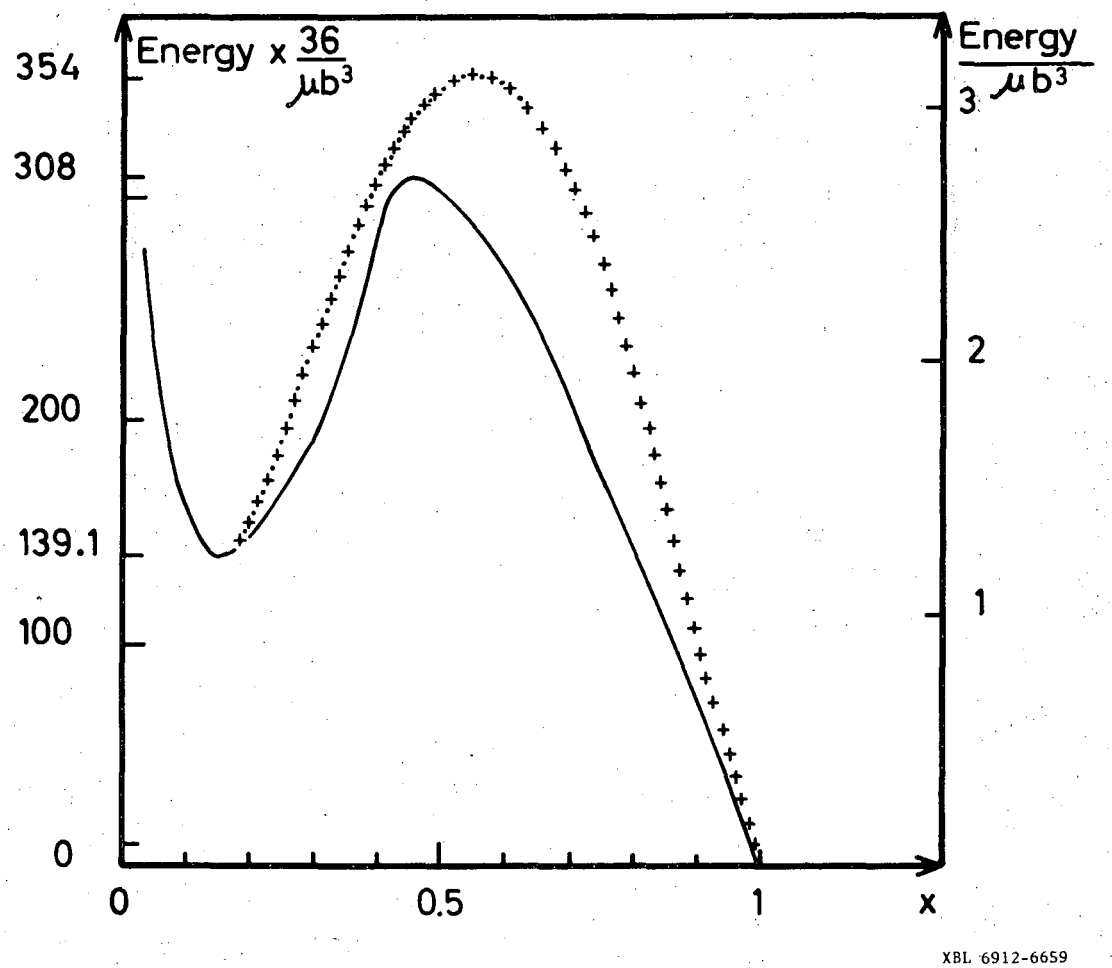
Energy x 36/μb³
354
308
200
139.1
100
0
0
0.5
1
x
Energy/μb³
3
2
1
XBL 6912-6659

fig. 10

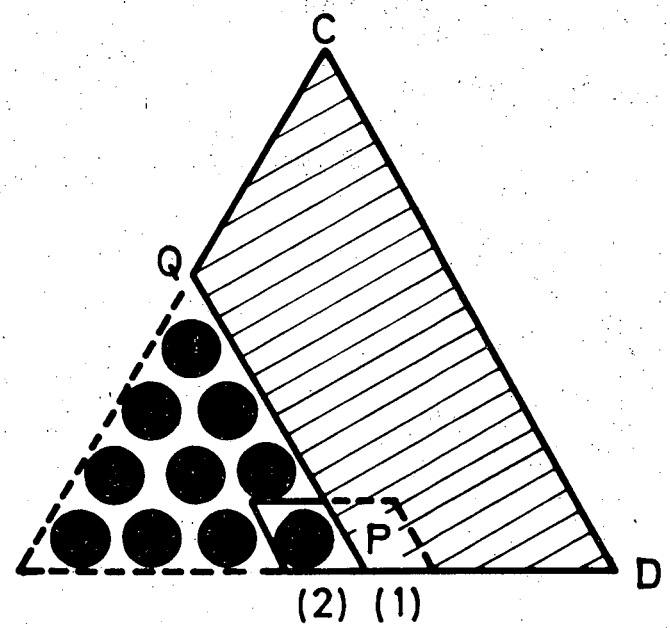

XBL 6912-6660

fig. 11

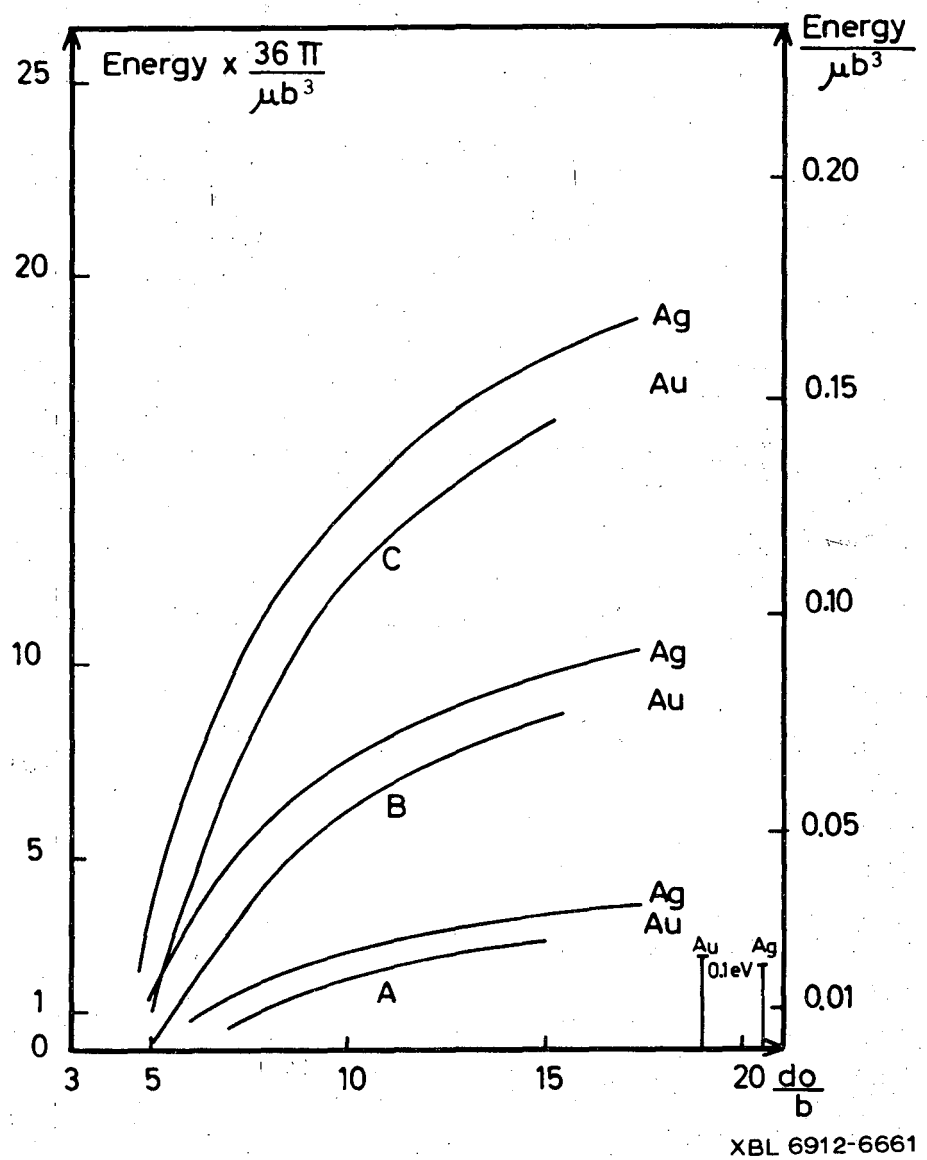
Energy x 36 π / μb³
Energy / μb³
25
20
10
5
1
0
0.20
0.15
0.10
0.05
0.01
Ag
Au
C
Ag
Au
B
Ag
Au
A
Au
Ag
0.1eV
3
5
10
15
20
do / b
XBL 6912-6661

fig. 12a

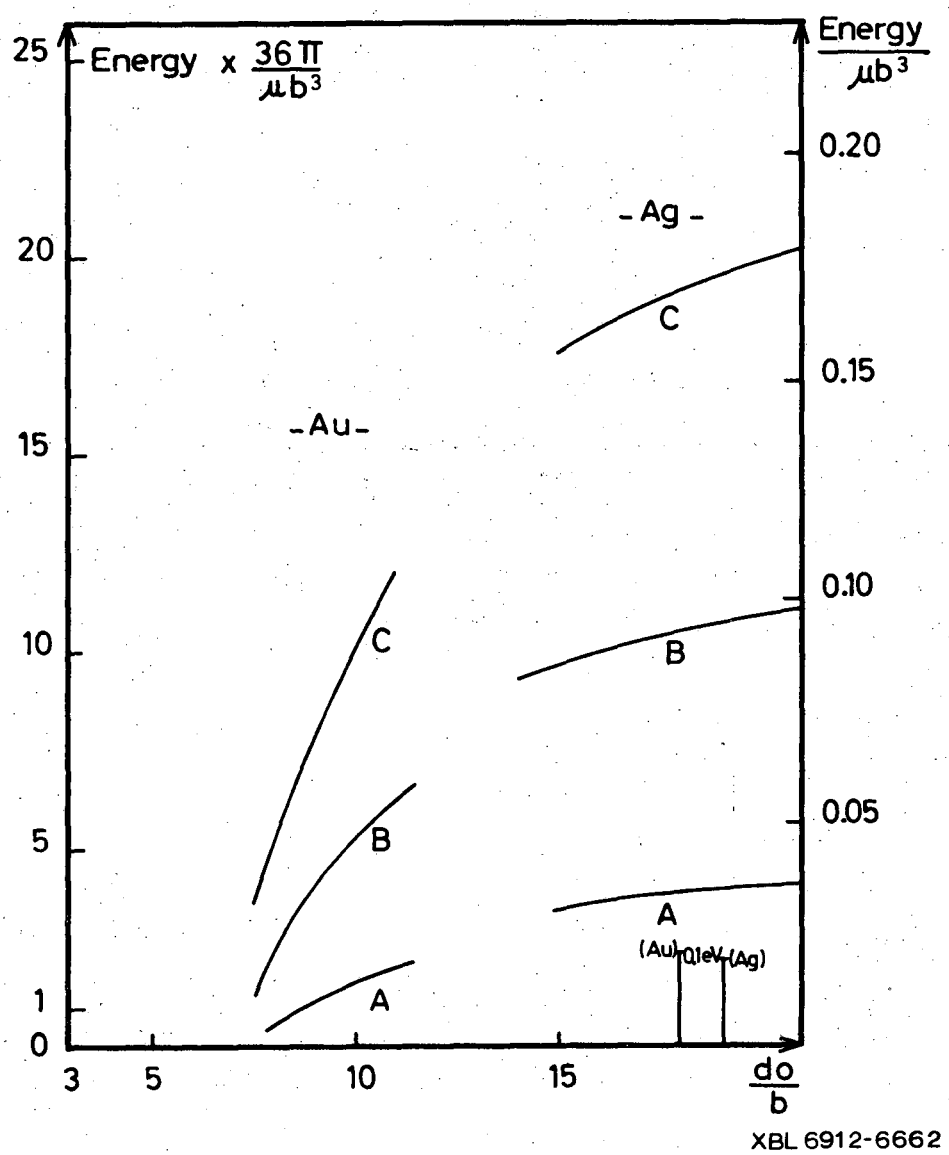
Energy x 36π/μb³
Energy/μb³
25
20
15
10
5
1
0
0.20
0.15
0.10
0.05
- Ag -
- Au -
C
B
A
(Au) 0.1eV (Ag)
3
5
10
15
do/b
XBL 6912-6662

fig. 12b

LEGAL NOTICE

This report was prepared as an account of Government sponsored work. Neither the United States, nor the Commission, nor any person acting on behalf of the Commission:

A. Makes any warranty or representation, expressed or implied, with respect to the accuracy, completeness, or usefulness of the information contained in this report, or that the use of any information, apparatus, method, or process disclosed in this report may not infringe privately owned rights; or

B. Assumes any liabilities with respect to the use of, or for damages resulting from the use of any information, apparatus, method, or process disclosed in this report.

As used in the above, "person acting on behalf of the Commission" includes any employee or contractor of the Commission, or employee of such contractor, to the extent that such employee or contractor of the Commission, or employee of such contractor prepares, disseminates, or provides access to, any information pursuant to his employment or contract with the Commission, or his employment with such contractor.

TECHNICAL INFORMATION DIVISION
LAWRENCE RADIATION LABORATORY
UNIVERSITY OF CALIFORNIA
BERKELEY, CALIFORNIA 94720